JOURNAL OF THERMOPHYSICS AND HEAT TRANSFER
Vol. 12, No. 3, July–September 1998

Thermal Contact Conductance for Aluminum and Stainless-Steel Contacts

E. E. Marotta*
Clemson University, Clemson, South Carolina 29634-0921
and
L. S. Fletcher†
Texas A&M University, College Station, Texas 77843-3123

In the present study, existing analytical models developed to predict the thermal contact conductance for both aluminum/aluminum and aluminum/stainless-steel surfaces in contact have been evaluated. The prediction of thermal contact conductance for these contacting pairs is difficult because a thin native oxide film generally occurs naturally on the aluminum materials. Therefore, one of the objectives of this study was to determine whether elastic or plastic thermal contact models could successfully predict both published and present experimental data for these commercially important alloys. A rigorous analytical analysis was conducted to check the validity of existing models (assuming either elastic or plastic deformation a priori) to predict the thermal contact conductance for nominally flat, uncoated aluminum surfaces in contact under vacuum conditions. Both elastic and plastic deformation models were compared with new unpublished experimental data for nominally flat, roughened surfaces.

Nomenclature

A = fraction of area in real contact
A_a = apparent area
a = contact spot radius, m
B_μ = microscopic gap number
b = flux tube radius, m
C_μ = microscopic constriction number
E = Young's modulus, N/m^2
E' = equivalent Young's modulus, N/m^2
f = elastoplastic function, $[1 + (6.5/\varepsilon^*)^2]^{0.5}/[1 + (13.0/\varepsilon^*)^{1/2}]^{1/1.2}$
$g(x)$ = constriction alleviation factor, Roess' formula
H = Vickers microhardness of softer substrate
H_μ = microscopic film number
h = thermal conductance, W/m^2 K
I_1 = integral, Ref. 7
J_0, J_1 = Bessel function, first kind
$K(\xi)$ = complete elliptic integral of modulus ξ
k_e = effective thermal conductivity
k_s = harmonic mean thermal conductivity, $2k_1k_2/(k_1 + k_2)$, W/m K
m, m_{abs} = mean absolute asperity slope, $m = (m_1^2 + m_2^2)^{1/2}$, m/m
m_0 = variance of surface heights, $\sigma^2 = \sigma_1^2 + \sigma_2^2$, μm^2
m_2 = variance of surface slopes, $m^2 = m_1^2 + m_2^2$, rad^2
m_4 = variance of second derivative of surface heights, μm^{-2}
P = apparent contact pressure, N/m^2
$\tan\theta$ = absolute asperity slope
U_μ = microscopic conductance number
u = mean plane separation, thermal contact conductance
$Z(\eta)$ = $(1/\sqrt{2\pi})\exp(-\eta^2/2)$
z = height above mean plane of surface, m
α_n = eigenvalues of Bessel function J_1
γ = index of deformation
ΔT_c = effective temperature drop across interface, K
δ = gap thickness
ε = b/a
ζ_n = roots of Bessel function $J_1(\zeta_n)$
η = number of asperities (peaks) per unit area, dimensionless separation
λ = eigenvalue, dimensionless mean plane separation
ν = Poisson ratio, dimensionless coordinate = (y/r_H)
σ = rms surface roughness, standard deviation
ς = thermal constriction parameter
Ω = $E'\sqrt{m_2/\pi}$

Subscripts
c = contact
e = elastic
i = index of summation
j = index of summation
p = plastic
1 = upper surface, material
2 = lower surface, material

Superscripts
$*$ = nondimensional parameter
$'$ = effective

Received Aug. 13, 1997; revision received Jan. 27, 1998; accepted for publication Jan. 28, 1998.

*Visiting Assistant Professor, Mechanical Engineering Department. Member AIAA.
†Thomas A. Dietz Professor, Conduction Heat Transfer Laboratory, Mechanical Engineering Department. Fellow AIAA.

I. Introduction

A REVIEW of the open literature indicates that a number of theoretical and experimental studies of the thermal contact conductance between two conforming, metallic surfaces have been conducted.[1–6] These theoretical studies of the flow of heat between solid bodies have been based on the consideration of heat flow through one microscopic contact region and the adjacent solid.

Cetinkale and Fishenden[1] assumed that the heat-flow lines at some distance far from the microscopic contact point between two metallic rods are parallel to the rod as well as to each other. As the interface is approached, the heat-flow lines converge toward the actual contact spots because the thermal conductivity of the metallic solid is much greater than that of

the surrounding interstitial fluid. They demonstrate that if two cylinders with different thermal conductivities are brought together, there exists an isothermal plane at the abutting surfaces. The heat flow can, therefore, be analyzed by considering only one of the two solid bodies with an imposed boundary condition of uniform temperature across the microscopic contact spot. However, because of the mixed boundary conditions of uniform temperature over part of the boundary (contact spot) and heat flux over the remainder, an exact solution was difficult. Although it is difficult to obtain an exact analytical solution because of the mixed boundary conditions, Clausing[2] was able to ascertain an exact numerical solution of the heat-flow pattern using the true boundary conditions.

Roess[3] and Mikic and Rohsenow[4] independently determined the thermal constriction resistance for a single isothermal contact spot at the center of the apparent contact area. References 3 and 4 derived similar approximate expressions for the thermal constriction resistance by replacing the isothermal contact boundary condition with a distributed heat-flux boundary condition. The assumed heat-flux distribution ensured that the contact spots were nearly isothermal; moreover, the revised boundary condition allowed an exact solution of the governing partial differential equation. The general expression derived for the thermal contact conductance of a single contact is

$$h_c = 2k_s \frac{c}{A_c} \frac{1}{\varsigma(c/b)} \tag{1}$$

where (c/b) is the constriction ratio, defined as the ratio of the contact radius to the flux radius. The thermal constriction parameter $\varsigma(c/b)$ compensates for the thermal effect of neighboring contact spots and can be calculated from the following expression:

$$\varsigma\left(\frac{c}{b}\right) = \frac{8}{\pi}\left(\frac{b}{c}\right) \sum \frac{\sin(\alpha_n c) J_1(\alpha_n c)}{(\alpha_n b)^3 J_0^2(\alpha_n b)} \tag{2}$$

A simple expression, which closely approximates the analytical and numerical solution, was given by Cooper et al.[5] as

$$\varsigma\left(\frac{c}{b}\right) = \left(1 - \frac{c_i}{b_i}\right)^{1.5} \tag{3}$$

which holds for the entire range of c_i/b_i.

Cooper et al. developed a correlation, with the assumption that the surface heights follow a Gaussian distribution, for multiple contact spots that included geometrical parameters such as surface roughness and surface asperity slope to predict thermal contact conductance. The dimensionless thermal contact conductance correlation was written as

$$\frac{h_c \sigma}{k_s |\tan \theta|} = 1.45 \left(\frac{P_a}{H}\right)^{0.985} \tag{4}$$

In addition to the plastic deformation theory developed by Cooper et al., other theories for plastic deformation of conforming, rough metals include those of Greenwood and Williamson[7] (modified elastic model) and Yovanovich,[8] which is a slight modification of Cooper et al.'s theory

$$\frac{h_c \sigma}{k_s m} = 1.25 \left(\frac{P_a}{H}\right)^{0.985} \tag{5}$$

Semiempirical correlations were introduced into Yovanovich's model by Song and Yovanovich[9] and Hegazy[10] to account for the increase in surface microhardness with decreasing depth of penetration of larger asperities. Specifically, Song and Yovanovich developed an explicit expression that permitted direct computation of the relative contact pressure and thermal joint conductance. The expression gave physical insights into the effect of the apparent pressure, surface roughness parameters, and the Vickers microhardness distribution upon the relative contact pressure. The relative contact pressure term in Eq. (4), P_a/H_c, was replaced with the following explicitly derived expression:

$$\frac{P}{H_c} = \left[\frac{P}{c_1\left(\frac{1.62 \times 10^6 \sigma}{m}\right)^{c_2}}\right]^{1/(1+\,0.071 c_2)} \tag{6}$$

Mikic[6] conducted a theoretical study that developed explicit expressions for the thermal contact conductance in cases where the surface asperities deformed purely elastically. For an asperity in contact with a rigid flat surface in purely elastic deformation, Mikic used the Hertzian theory to write an expression for the thermal contact conductance

$$h_e = 1.55 \frac{k_s \tan \theta}{\sigma} \left(\frac{P\sqrt{2}}{E'|\tan \theta|}\right)^{0.94} \tag{7}$$

where the fraction of actual area in contact because of elastic deformation of the surface asperities is

$$A = \frac{P\sqrt{2}}{E'|\tan \theta|} \tag{8}$$

Mikic also developed explicit expressions for the thermal contact conductance where the surface asperities deform plastically while the underlying substrate deforms elastically. With the correction for elastic deformation of the underlying substrate and plastic deformation of surface asperities, Mikic modified the thermal contact conductance equation to include the following correction:

$$h_p^* = \frac{Z(Q^{-1}[1 + 2.5\gamma^{1.2}]P_p)}{2(1 + 1.05\gamma)(1 - \sqrt{P_p})^{1.5}} \tag{9}$$

where P_p represents the dimensionless actual contact pressure for plastic deformation. The parameter γ is an index of deformation that is predominantly elastic for γ greater than or equal to 3.0 and predominantly plastic for γ less than 0.33. The dimensionless actual contact pressure is equal to the fraction of actual area by the following expression:

$$P_p = A = \tfrac{1}{2}\operatorname{erfc}(\eta/\sqrt{2}) = Q(\eta) \tag{10}$$

with the actual contact pressure for plastic deformation assumed to be equal to the microhardness of the softer material in contact

$$P_p = P_a/H \tag{11}$$

Bush and Gibson[11] treated an isotropic rough surface statistically, such that the geometric parameters are specified in terms of power-spectra moments. With the use of these surface moments, expressions for the nondimensional variables of the contact spot radius a^*, the flow channel b^*, and the thermal contact conductance h^* were developed as

$$a^* = \frac{a}{\sqrt{2}(3m_0/m_4)^{1/4}} \tag{12}$$

$$b^* = \frac{b}{\sqrt{2}(3m_0/m_4)^{1/4}} \tag{13}$$

$$h^* = \frac{C_s}{(\sqrt{2}k_s/\pi)(m_4/3m_0)^{1/4}} \tag{14}$$

where the thermal contact conductance was obtained from the reciprocal of the thermal contact resistance R_s

$$C_s = \frac{2k_m x}{\pi b g(x)} \tag{15}$$

Bush and Gordon's analysis showed that the dimensionless thermal contact conductance for plastic asperity deformation with applied apparent pressure could be written as

$$C_p^* = 2.13(P/M)^{0.94} \tag{16}$$

$$C_e^* = 1.31(P/\Omega)^{0.89} \tag{17}$$

Other theories for elastic deformation of conforming, rough metals include those of Greenwood and Williamson,[7] Whitehouse and Archard,[12] Bush et al.,[13] and Blahey et al.[14] Blahey et al.'s model incorporated the radius of curvature of the deforming asperity peaks for the prediction of thermal contact conductance.

Sridhar and Yovanovich[15] compared these elastic and plastic deformation models to controlled experiments conducted by Hegazy,[10] Antonetti,[16] and McWaid,[17] and concluded that the thermal contact conductance model developed by Yovanovich[8] was the most successful for the prediction of experimental data for conforming, rough metals.

Sridhar and Yovanovich[18] developed a model whose basis is on the work conducted by Cooper et al.[5] in their plastic model, but differs in the deformation aspects of the thermal contact conductance model. The model covers the entire range of material behavior from elastic to fully plastic deformation as well

Table 1 Analytical models and correlations for thermal contact conductance of bare contacts

Reference	Analytical model/correlation	Comments
Cetinkale and Fishenden[1]	$\frac{h_{c+g,s}\sigma}{km} = \frac{k_f\sigma}{\lambda km} + \frac{\sigma a_s}{m b_s^2 \tan^{-1}[(b_s/a_s)\sqrt{1 - (k_f/h\lambda)} - 1]}$ $\lambda = 0.61(\sigma_{1,R_2} + \sigma_{2,R_2})$ $b_s = 0.0048(\mathrm{TIR}_1 + \mathrm{TIR}_2) \times (P_{\max}^{0.33} \times P^{0.66}/H_M)^{0.5}$; elastic $b_s = 0.0048(\mathrm{TIR}_1 + \mathrm{TIR}_2) \times (P/H_M)^{0.5}$; plastic	Flat, rough surface Similar metals Contact and gap conductance—air, oil, and alcohol gap filters TIR = true indicator reading
Mikic and Rohsenow,[4] plastic deformation	$\frac{h_{c,s}\sigma}{mk} = 0.90\left(\frac{P}{H_v}\right)^{0.941}$	Optically or nominally flat, rough surfaces
Cooper et al.,[5] plastic deformation	$\frac{h_{c,s}\sigma}{km} = \frac{1}{2\sqrt{2\pi}} \frac{\exp(u^*2/2)}{[1 - \sqrt{0.5\,\mathrm{erfc}(u^*/\sqrt{2})}]^{1.5}}$ $\frac{h_{c,s}\sigma}{km} = 1.45\left(\frac{P}{H_v}\right)^{0.985}$	Nominally flat, rough surfaces Dimensionless pressure (P/H) 3.6×10^{-4} to 1.0×10^{-2} Roughness 1.0–8.0 μm Asperity slope 0.08–0.16 rad
Greenwood and Williamson,[7] plastic deformation	$\frac{h_{c,s}\sigma}{mk} = 2\frac{\sigma}{m} \frac{\eta\sqrt{\mathrm{erfc}(u^*/\sqrt{2})\sigma\beta I_1(u^*)}}{[1 - \sqrt{\eta 2\pi\sigma\beta I_1(u^*)}]^{1.5}}$ $\frac{h_{c,s}\sigma}{mk} = C_1\left(\frac{P}{H_v}\right)^{0.98}$	Optically or nominally flat, rough surfaces $C_1 = 1.91$, $\alpha = 15$ $C_2 = 1.51$, $\alpha = 5$
Mikic,[6] elastic deformation	$\frac{h_{c,s}\sigma}{km} = \frac{1}{4\sqrt{\pi}} \frac{\exp(u^*2/2)}{[1 - \sqrt{0.25\,\mathrm{erfc}(u^*/\sqrt{2})}]^{1.5}}$ $\frac{h_{c,s}\sigma}{km} = 1.55\left(\frac{\sqrt{2}P}{E'm}\right)^{0.98}$ Fraction of actual area $= A = \frac{P\sqrt{2}}{E' \tan\theta}$	Nominally flat, rough surfaces Dimensionless pressure (P/H_c) 3.6×10^{-4} to 1.0×10^{-2} Roughness 1.0–8.0 μm Asperity slope 0.08–0.16 rad
Bush and Gibson,[11] elastic deformation	$h^* = \frac{C_s}{(\sqrt{2}k_s/\pi)(m_4/3m_0)^{0.25}}$ $C_s = \frac{2k_m x}{\pi b g(x)}$ $h_e^* = 1.31\left(\frac{P}{\Omega}\right)^{0.89}$ correlation	Isotropic, rough surfaces Geometric parameters are specified in terms of moments of its power spectra
Blahey et al.,[14] elastic deformation	$\frac{h_{c,s}\sigma}{km} = \frac{2C_2}{mC_1}\left(\frac{\sigma}{\beta}\right)^{(1-C_3)/2}\left(\frac{P}{E}\right)^{C_3}$	Flat, rough surfaces $0.05 \le C_1 \le 0.10$ $3.63 \le 2C_2 \le 4.85$ $0.93 \le C_3 \le 0.95$
Greenwood and Williamson,[7] elastic deformation	$\frac{h_{c,s}\sigma}{mk} = \sqrt{2}\frac{\sigma}{m} \frac{\eta\sqrt{\mathrm{erfc}(u^*/\sqrt{2})\sigma\beta I_1(u^*)}}{[1 - \sqrt{\eta\pi\sigma\beta I_1(u^*)}]^{1.5}}$ $\frac{h_{c,s}\sigma}{km} = C_1\left(\frac{\sqrt{2}P}{E'm}\right)^{0.98}$	Optically or nominally flat, rough surfaces $C_1 = 1.87$, $\alpha = 15$ $C_2 = 1.75$, $\alpha = 5$
Onions and Archard,[19] elastic deformation	$\frac{h_{c,s}\sigma}{mk} = \frac{2}{5\Delta 5}\frac{\sigma}{m} \frac{\sqrt{I_{0.0}(u^*)I_1(u^*)}}{[1 - \sqrt{0.2\pi I_{1,1}(u^*)}]^{1.5}}$ $\frac{h_{c,s}\sigma}{km} = C_1\left(\frac{\sqrt{2}P}{E'm}\right)^{0.97}$	Optically or nominally flat, rough surfaces $C_1 = 2.80$, $\alpha = 60$ $C_2 = 2.38$, $\alpha = 4$ Reformulated Whitehouse and Archard[12] model

as deformation in between, which they denote as elastoplastic deformation. A nondimensional strain parameter e_c was introduced that is similar to the deformation index developed by Mikic,[6] except that the hardness parameter H is replaced by a yield/flow stress parameter S_f and a numerical constant appears. With the incorporation of the yield/flow stress parameter, the dimensionless thermal contact conductance equation becomes

$$h_c = \frac{1}{2\sqrt{2\pi}} \frac{\sqrt{f_{ep}} \exp[-(\lambda^2/2)]}{[1 - \sqrt{(f_{ep}/2)}\mathrm{erfc}(\lambda/2)]^{1.5}} \qquad (18)$$

The parameter λ is the dimensionless surface mean plane separation, and f_{ep} is a function that indicates whether the deformation regime is elastic, elastoplastic, or plastic as determined by the yield or flow stress of the material. This model was developed to explain moderate differences between Yovanovich's[8] theory and experiments conducted at low apparent interface contact pressures.

A summary of the analytical expressions developed for the prediction of thermal contact conductance or contact resistance for uncoated metallic surfaces in contact is shown in Table 1. An elastic deformation model by Onions and Archard[19] has also been included in the table for reference.

II. Experimental Program

To provide data for the development of a theoretical analysis of uncoated Al/Al (aluminum 6101-T6-T61/aluminum A356-T61) and Al/SS (aluminum 6101-T6/stainless-steel 304) surfaces in contact, an experimental investigation was conducted. To determine the effect on thermal contact conductance for nominally flat, uncoated surfaces of dissimilar alloys, the mean interface temperature, apparent interface pressure, and vacuum environment were controlled. Hence, the existing experimental facility was modified to provide these testing conditions and accuracy. The experimental apparatus consists of the test chamber, interface pressure and temperature control instrumentation, vacuum environment control system, and the data collection system. A description of the experimental facility and its design will be discussed along with the associated instrumentation. Further, the test procedure and test program will be presented along with an uncertainty analysis.

The experimental test chamber employed in this investigation consists of a vertical column consisting of a frame with sliding plates for supporting two combination heat-source/sink-specimen-holder assemblies, the test samples, a load cell, and pneumatic bellows, as shown in Fig. 1. A uniform contact pressure over the test interface was assured by the use of two hardened steel balls that transfer load from the frame to the source-sink-holder assemblies and, in turn, to the specimens. Flexible neoprene hoses were employed to supply coolant to the holder assemblies to eliminate lateral loads that might contort the vertical column and skew the pressure distribution over the interface surfaces.

The experimental test facility is housed in a vacuum environment where a pressure of 1×10^{-5} torr was attained by a Varian VHS-6 oil diffusion pump backed by an Alcatel 2300 two-stage rotary roughing pump. The vacuum pressure was monitored by thermocouple and filament gauges connected to a Perkin Elmer Monitorr 300 instrument.

Each of the test samples was instrumented with five special "limit of error" (1.1°C) K-type thermocouples (AWG 30) inserted into 0.16-cm- (0.064-in.-) diam holes drilled radially to the specimen axes at 0.635-cm (0.25-in.) intervals. High thermal conductivity, boron nitride adhesive cement was then tamped into the holes to ensure good thermal contact of the thermocouple beads to the side of the holes. The thermocouples were connected to a Hewlett Packard 3497A data-acquisition unit, which communicated through software with an IBM-compatible personal computer. The applied axial contact force on the test column was applied by pressurizing the bellows, and the contact load was monitored by a load cell and signal amplifier. The load cell system was calibrated by static loading with known weight and then compensated for the vacuum condition prior to the activation of the experimental computer program.

The thermal contact conductance specimens and flux-meters are each 2.54 cm (1.0 in.) in diameter. The upper and lower flux-meter specimens are 10.16 cm (4.0 in.) long and are fabricated from aluminum alloy 6101-T6 and stainless-steel 304, respectively, whereas the center test specimen is 3.81 cm (1.5 in.) long and is machined from aluminum A356-T61 alloy and stainless-steel 304. Each end surface for the aluminum 6101-T6 and aluminum A356-T61 alloys were subsequently lapped and mechanically polished to obtain a surface roughness of less than 1 μm (40 μin.). Three sets of specimens were fabricated and mechanically processed to show repeatability of measured experimental results.

Successive tests were conducted with surface characteristics of varying roughness. Each test began with insertion of the selected middle specimen of varying roughness (aluminum A356-T61 or stainless-steel 304) between the upper and lower flux-meters. A special fixture was clamped around the column of three specimens to ensure exact coaxial mating of the surfaces. A light load was applied and the alignment fixture was then removed. A preload was not applied for these tests. The bell jar was sealed over the vertical column apparatus and a vacuum was drawn. Power was supplied to the heater, which was located on the source-sink-holder assembly, and coolant was pumped through the opposite assembly.

Experimental data were again obtained utilizing a Hewlett Packard data logger that was controlled through software by a personal computer via an IEEE-488 bus. The temperature gradients and thermal conductivities of the heat flux-meters were used to determine the heat fluxes in both the upper and lower flux-meters. The temperature change across the aluminum 6101-T6 and aluminum A356-T61 or stainless-steel 304 interface was determined by extrapolating the thermal gradient in the flux-meters to the bare junction surface.

The reported thermal contact conductance data are for the case of heat flux passing from the aluminum 6101-T6 flux-meter to the bare aluminum A356 or stainless-steel specimen. The experimental investigation was conducted at apparent contact pressures of 172–4128 kPa (25–600 psi) and mean interface temperatures of 60 and 80°C (140 and 176°F, respectively). The experimental results include the thermal contact

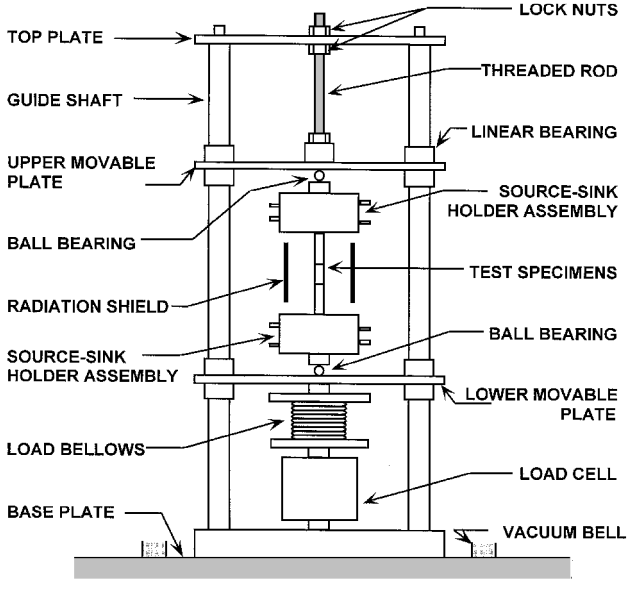

Fig. 1 Schematic of the test fixture.

conductance for each surface pair over the range of pressures and mean temperatures investigated.

Accuracy of temperature readings is critical in estimating the overall uncertainty associated with the calculated thermal contact conductance. The average temperatures of each fluxmeter, specimen, and calibration standard materials are required in determining their thermal conductivity as a function of temperature. These material conductivities are required for tabulating the heat flux in the test column. The type-K thermocouples used in the present investigation have a special limit of error rating, which defines the maximum difference between the reading and true temperature to be the greater of 1.1 K or 0.4% above 0°C.

On the basis of the uncertainty in temperature readings and the relative variation of the thermal conductivity of the calibration standard, i.e., 0.12% for electrolytic iron, the overall relative uncertainties in the specimen thermal conductivities are 2.46% for aluminum A356-T61, 2.76% for aluminum 6101-T6, and 1.98% for stainless-steel 304.

The change in temperature between the instrumented locations of a specimen is the increment to which the variance of the individual temperature readings must be compared to obtain an estimate of the uncertainty in the temperature gradient. The average changes in temperature between instrumented locations for the substrate materials employed in this present study ranged from 0.2 K for aluminum 6101-T6 to 5.0 K for stainless-steel 304. For the present investigation, the uncertainty in the temperature gradient ranged from 8.87% for aluminum A356-T61 to 1.42% for stainless-steel 304. A rigorous analysis of the uncertainty calculations can be found in Marotta.[20]

III. Results and Discussion

Any analytical model that predicts the thermal contact conductance or resistance of a coated metallic surface in contact with an uncoated surface must first be able to predict the thermal contact conductance when both surfaces are uncoated. To ascertain this requirement, an extensive experimental program,

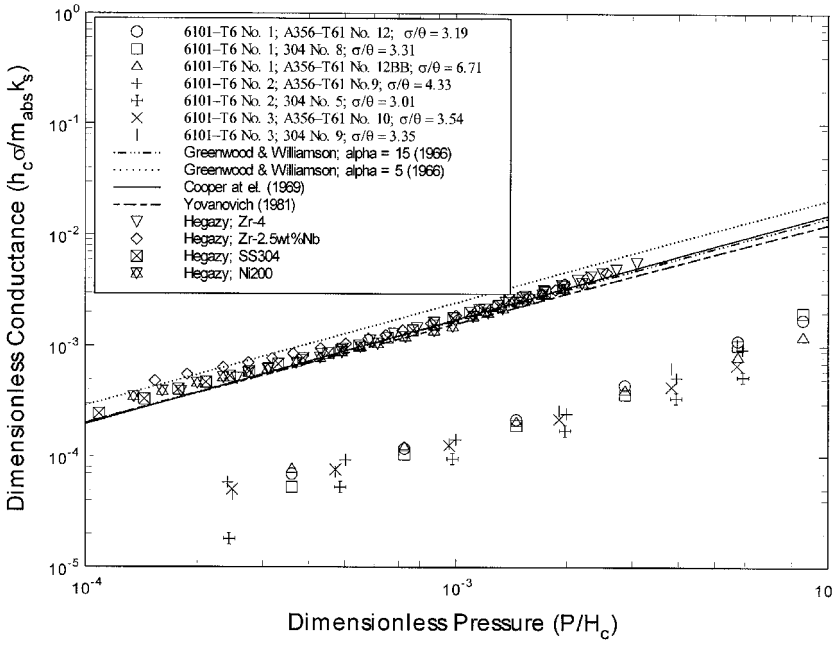

Fig. 2 Comparison of plastic deformation models to experimental data for uncoated aluminum and stainless-steel specimens.

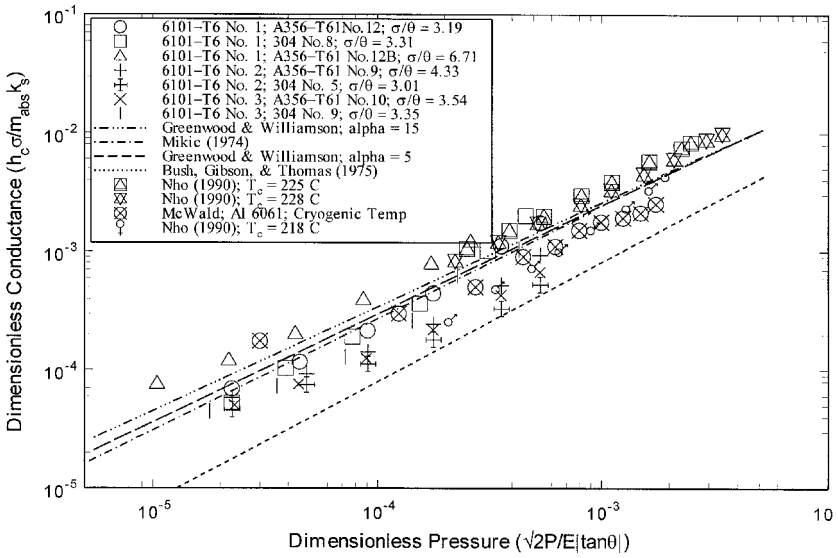

Fig. 3 Comparison of elastic deformation models to experimental and published data for uncoated aluminum and stainless-steel specimens.

which employed carefully prepared and specified contact surfaces, was undertaken with strictly controlled conditions. The prediction of thermal contact conductance for similar aluminum surfaces or dissimilar surfaces in contact presents a unique obstacle because a thin native oxide film generally occurs on most aluminum materials naturally.

A rigorous analytical analysis was conducted to check the validity of existing models (assuming either plastic or elastic deformation a priori) to predict the thermal contact conductance for nominally flat, uncoated aluminum surfaces in contact under vacuum conditions. Elastic deformation models developed by Mikic,[6] Greenwood and Williamson,[7] and Bush et al.,[13] and plastic deformation models developed by Cooper et al.,[5] Greenwood and Williamson,[7] and Yovanovich[8] were compared with the experimentally measured data.

Figures 2 and 3 present the dimensionless thermal contact conductance h^* as a function of dimensionless pressure (P/H_c or $\sqrt{2}P/E'|\tan\theta|$). These are suitable candidates for the values of dimensionless contact pressures based on the work conducted by Cooper et al.[5] and Mikic,[6] respectively. The comparisons between existing plastic and elastic models and the experimental data obtained in this investigation are respectively, shown. The roughness and asperity mean absolute slope for each specimen pair were measured prior to testing and are presented as the ratio σ/θ in Figs. 2 and 3. This ratio σ/θ is a critical parameter, essential for predicting the thermal contact conductance. The values for the ratio ranged from 3.01 to 4.33 for the specimen pairs that were lapped and mechanically polished. A single specimen pair that was roughened by bead blasting for increased surface roughness is also included for comparison. The ratio σ/θ had a value of 6.71.

As can be seen from Figs. 2 and 3, the elastic deformation models compare more favorably with the measured and published thermal contact conductance data than the plastic deformation models. The predicted values for the plastic deformation models were at least one order of magnitude higher

Table 2 Comparison between the predicted values and the experimental data for dimensionless thermal contact conductance

Material pair	Model	Maximum, %	rms, %
Aluminum 6101-T6 no. 1	Mikic[5]	−24.86	16.22
Aluminum A356-T61 no. 12	Greenwood and Williamson[7]	53.42	38.57
Aluminum 6101-T6 no. 1	Mikic	−34.41	28.65
Stainless-steel 304 no. 8	Greenwood and Williamson	72.68	62.80
Aluminum 6101-T6 no. 1	Mikic	20.35	14.89
Aluminum A356-T61 no. 12B	Greenwood and Williamson	61.53	49.35
Aluminum 6101-T6 no. 2	Mikic	89.92	66.34
Aluminum A356-T61 no. 9	Greenwood and Williamson	154.51	120.32
Aluminum 6101-T6 no. 2	Mikic	171.07	138.70
Stainless-steel 304 no. 5	Greenwood and Williamson	248.70	213.96
Aluminum 6101-T6 no. 3	Mikic	112.86	98.44
Aluminum A356-T61 no. 10	Greenwood and Williamson	185.25	162.81
Aluminum 6101-T6 no. 3	Mikic	90.74	70.15
Stainless-steel 304 no. 9	Greenwood and Williamson	156.01	127.56
Nho[24]	Mikic	−38.00	36.30
Aluminum 6061-T6 ground to lap	Greenwood and Williamson	217.14	181.78
Nho[24]	Mikic	−30.49	8.20
Aluminum 6061-T6 lap to ground	Greenwood and Williamson	−43.93	36.84
Nho[24]	Mikic	96.58	53.71
Aluminum 6061-T6 lap to ground	Greenwood and Williamson	58.12	30.42
Stainless-steel 304 McWaid[17]	Mikic	63.55	21.18
Aluminum 6061	Greenwood and Williamson	−63.05	31.89

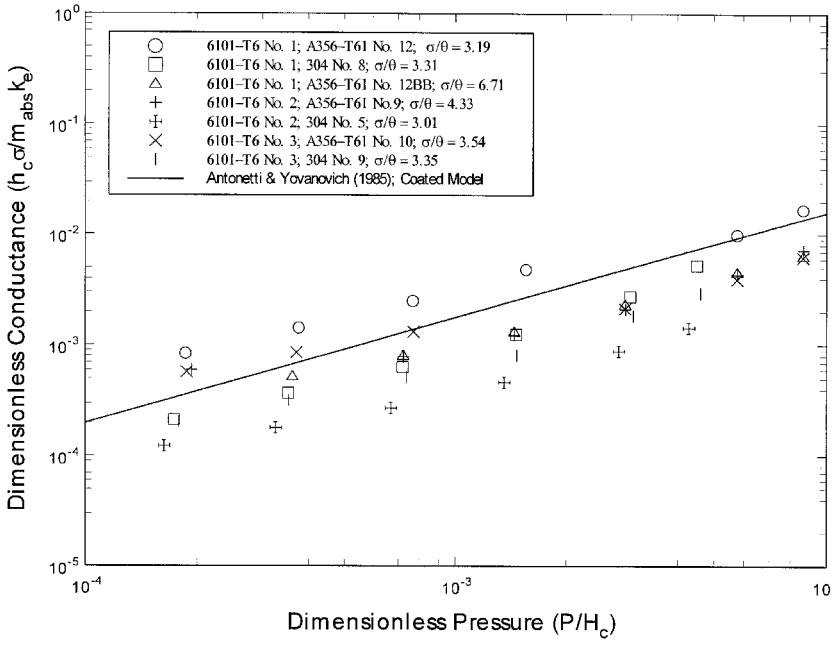

Fig. 4 Comparison of coated plastic model to experimental data for an assumed coated aluminum substrate.

than the measured experimental data, whereas the difference between the experimental and published data is much less for the elastic deformation models.

While all of the measured and published experimental data do not lie precisely on the predictive curves, the trend for the majority of the data is better predicted by the elastic deformation models. The deviation for several specimen pairs, which involved uncoated aluminum alloy in contact with uncoated stainless steel, was quite large when compared to the model curves. However, if one takes into consideration that the average overall uncertainty in thermal contact conductance for uncoated aluminum 6101-T6 to aluminum A356-T61 and for uncoated aluminum 6101-T6 to stainless-steel 304 junctions was 16.00 and 12.00%, respectively, the correlation is quite good. A summary of the calculated maximum and rms % differences is shown in Table 2 for each specimen pair tested, which were compared to the values predicted by the elastic deformation models developed by Mikic[6] and Greenwood and Williamson[7] (Figs. 2 and 3). It must be noted that these models do not take into account the oxide film present on the surfaces and, thus, the predicted dimensionless conductance is not compensated for this added complexity. This may cause some of the high differences in maximum and rms % values.

There is an astounding observation that both Figs. 2 and 3 clearly show: Surface asperities for aluminum surfaces appear to undergo elastic deformation rather than plastic deformation when in contact. According to the deformation index γ developed by Mikic,[6] aluminum surfaces should undergo plastic deformation ($\gamma < 0.30$) instead of elastic deformation ($\gamma > 3.0$). The deformation index value calculated for the aluminum pairs of the present investigation was $\gamma = 0.023$, which indicates plastic deformation predominates. Therefore, if only bulk material properties are considered for aluminum surfaces in contact, this analysis disproves any conception that aluminum surface asperities should deform plastically.

The ambiguity of elastic asperity deformation for aluminum surfaces becomes clear when the presence of a thin native oxide film is considered. An oxide film on aluminum is primarily aluminum oxide (Al_2O_3), which possesses a higher Young's modulus (~300–500 GPa) and compressive yield strength than metallic aluminum. Previous researchers such as Yip[21] and Al-Astrabadi et al.[22] have shown that thicknesses between 0.075 and 0.236 μm can be either artificially or naturally present on aluminum surfaces. These film thicknesses will have little effect on surface topographies but will have a significant impact on surface asperity deformation that manifests itself in the measured thermal contact conductance.

The ability to predict the experimental thermal contact conductance data with the use of a plastic model, which has a native oxide present, was investigated. That is, if the native oxide was the major contributor to the influence on the thermal contact conductance data, then a plastic model modified for the present of the native oxide film should be able to predict the experimental measured data, i.e., where the major assumption is plastic deformation of the surface asperities. Assumptions for film thickness, hardness, and thermal conductivity were made because these parameters are difficult to obtain because of the physical size of the film, i.e., thicknesses between 0.075 and 0.236 μm. The model developed by Antonetti and Yovanovich[23] for coated surfaces was employed with an assumed film thickness of 0.1 μm, a film hardness equal to 2.94 GPa, i.e., H_v 300 kg/mm^2; and a thermal conductivity of 0.72 W/m-K. An effective thermal conductivity k_e for the film/substrate combination was calculated based on the expression developed by Antonetti and Yovanovich for coated surfaces. The effective microhardness, which is required in the model developed by Antonetti and Yovanovich, was calculated from the expressions developed by Marotta.[20]

Note in Fig. 4 that the experimental data presented in Fig. 2, which show significant deviation from the plastic models, have less deviation from the modified Antonetti and Yovanovich plastic model for coated surfaces. While the inclusion of a film effect seems to improve the correlation between the experimental data and the model, the experimental data also exhibited increased scatter when compared to Fig. 2. This increased scatter may be attributed to the differences in predicted effective microhardness between the data sets, but another mechanism may also be influential. In fact, implicit in the present model is the assumption that the asperities of the harder material penetrate the softer material. However, for materials that may have similar microhardness values, this concept may not apply and some combination of microhardness may be needed. Experimental data from Nho[24] for anisotropic surfaces have been included for comparison to the elastic models.

IV. Conclusions and Recommendations

In conclusion, the coverage of aluminum surface asperities with a thin native oxide film can have a significant impact on surface deformation mechanics and thermal contact conductance. From this experimental investigation and published data it is evident that an elastic thermomechanical model would best predict the microscopic thermal contact resistance for nonflat, roughened aluminum surfaces. Therefore, models developed for nonflat, nonmetallic-coated aluminum surfaces in contact must include an elastic deformation parameter for microscopic contact resistance. A rigorous analytical analysis was conducted to check the validity of these existing models to new unpublished and existing experimental data.

Acknowledgments

Partial support for this investigation was provided by the Office of Naval Research Grant N00014-95-1-0842 and the Texas Engineering Experiment Station Center for Space Power.

References

[1]Cetinkale, T. N., and Fishenden, M., "Thermal Conductance of Metal Surfaces in Contact," *International Conference of Heat and Mass Transfer*, Inst. of Mechanical Engineering, London, 1951, pp. 271–275.

[2]Clausing, A. M., "Heat Transfer at the Interface of Dissimilar Metals—The Influence of Thermal Strain," *International Journal of Heat and Mass Transfer*, Vol. 9, No. 5, 1966, pp. 791–801.

[3]Roess, L. C., "Theory of Spreading Conductance," Appendix to Weills, N. D., and Ryder, E. A., "Thermal Resistance Measurements on Joints Formed Between Stationary Metal Surfaces," Semi-Annual American Society of Mechanical Engineers Heat Transactions Division Meeting, Milwaukee, WI, 1948.

[4]Mikic, B. B., and Rohsenow, W. M., "Thermal Contact Resistance," Massachusetts Inst. of Technology, Mechanical Engineering Dept., Cambridge, MA, TR 4542-41, Sept. 1966.

[5]Cooper, M. G., Mikic, B. B., and Yovanovich, M. M., "Thermal Contact Conductance," *International Journal of Heat and Mass Transfer*, Vol. 12, Jan. 1969, pp. 279–300.

[6]Mikic, B. B., "Thermal Contact Conductance; Theoretical Considerations," *International Journal of Heat and Mass Transfer*, Vol. 17, Aug. 1974, pp. 205–214.

[7]Greenwood, J. A., and Williamson, J. B. P., "Contact of Nominally Flat Surfaces," *Proceedings of the Royal Society of London, Series A: Mathematical and Physical Sciences*, Vol. 295, 1966, pp. 300–319.

[8]Yovanovich, M. M., "Overall Constriction Resistance Between Contacting Rough, Wavy Surfaces," *International Journal of Heat and Mass Transfer*, Vol. 12, No. 10, 1969, pp. 1517–1520.

[9]Song, S., and Yovanovich, M. M., "Explicit Relative Contact Pressure Expression: Dependence Upon Surface Roughness Parameters and Vickers Microhardness Coefficients," *Journal of Thermophysics and Heat Transfer*, Vol. 2, No. 1, 1987, pp. 43–47.

[10]Hegazy, A. A., "Thermal Joint Conductance of Conforming Rough Surfaces: Effects of Surface Microhardness Variations," Ph.D. Dissertation, Univ. of Waterloo, ON, Canada, 1985.

[11]Bush, A. W., and Gibson, R. D. "A Theoretical Investigation of Thermal Contact Conductance," *Applied Energy*, Vol. 5, No. 1, 1979, pp. 11–22.

[12]Whitehouse, D. J., and Archard, J. F., "The Properties of Random Surfaces of Significance in Their Contact," *Proceedings of the Royal*

Society of London, Series A: Mathematical and Physical Sciences, Vol. 316, 1970, pp. 97–121.

[13]Bush, A. W., Gibson, R. D., and Thomas, T. R., "The Elastic Contact of a Rough Surface," *Wear*, Vol. 35, 1975, pp. 87–111.

[14]Blahey, A., Tevarrwerk, J. L., and Yovanovich, M. M., "Contact Conductance Correlations of Elastic Deforming Flat Rough Surfaces," AIAA Paper 80-1470, Jan. 1980.

[15]Sridhar, M. R., and Yovanovich, M. M., "Critical Review of Elastic and Plastic Thermal Contact Conductance Models and Comparison with Experiment," AIAA Paper 93-2776, July 1993.

[16]Antonetti, V. W., "On the Use of Metallic Coatings to Enhance Thermal Contact Conductance," Ph.D. Dissertation, Univ. of Waterloo, ON, Canada, 1983.

[17]McWaid, T. H., "Thermal Contact Resistance Across Pressed Metal Contact in a Vacuum Environment," Ph.D. Dissertation, Univ. of California, Santa Barbara, CA, 1990.

[18]Sridhar, M. R., and Yovanovich, M. M., "Elastoplastic Constriction Resistance of Sphere/Flat Contacts: Theory and Experiment," *ASME Winter Annual Meeting* (New Orleans, LA), HTD-Vol. 263, 1994, pp. 123–134.

[19]Onions, R. A., and Archard, J. F., "The Contact of Surfaces Having a Random Structure," *Journal of Physics, D: Applied Physics*, Vol. 6, 1973, pp. 289–304.

[20]Marotta, E., "Thermal Contact Conductance of Non-Flat, Non-Metallic, Isotropic Roughened Coated Surfaces: Analytical and Experimental Investigation," Ph.D. Dissertation, Texas A&M Univ., College Station, TX, 1997.

[21]Yip, F. C., "Effect of Oxide Films on Thermal Contact Resistance," AIAA Paper 74-693, July 1974.

[22]Al-Astrabadi, F. R., O'Callaghan, P. W., and Probert, S. D., "Thermal Resistance of Contacts: Influence of Oxide Film," AIAA Paper 80-1467, Jan. 1980.

[23]Antonetti, V. W., and Yovanovich, M. M., "Enhancement of Thermal Contact Conductance by Metallic Coatings: Theory and Experiment," *Journal of Heat Transfer*, Vol. 107, Aug. 1985, pp. 513–519.

[24]Nho, K. M., "Experimental Investigation of Heat Flow Rate and Directional Effect on Contact Conductance of Anisotropic Ground/Lapped Interfaces," Ph.D. Dissertation, Univ. of Waterloo, ON, Canada, 1990.